CONTROL OF ROTORDYNAMIC INSTABILITY IN A TYPICAL GAS TURBINE'S POWER ROTOR SYSTEM

Nicholas M. Veikos, Richard H. Page, and Edward J. Tornillo
AVCO Lycoming Division
Stratford, Connecticut 06497

In the study of rotor systems operating above the first critical speed, it is important to include the effect of rotor internal friction on the system's stability. This internal friction is commonly caused by sliding press fits or sliding splines. Under conditions of high speed and low bearing damping, these systems will occasionally whirl at a frequency less than the shaft's rotational speed. This subsynchronous precession is a self-excited phenomenon, and unlike synchronous precession, stress reversals are created. Since the mid-sixties this phenomenon was observed during engine testing, and analysis has pointed the way for successful attenuation of the problem. The reduction of spline friction and/or the inclusion of squeeze film damping have controlled the instability. This case history along with the detail design of the squeeze film dampers will be discussed.

INTRODUCTION

It is not unusual for present day gas turbine rotor systems to operate above several rigid body critical speeds. These are critical speeds at which most of the deflection and strain energy is in the bearings and bearing supports while the shaft itself moves essentially as a rigid body. Modern balancing techniques and bearing designs permit the rotors to pass through these critical speeds during startup or shutdown, experiencing only a nominal increase in vibration levels at the resonance points. However, it cannot be assumed that the rotor design is satisfactory simply because it allows the system to run through critical speeds. When the rotor is operating in the supercritical regime, it is important to consider the possibility of rotor vibration caused by forces other than unbalance excitation.

One such type of vibration is nonsynchronous precession due to shaft internal friction caused by sliding splines or press fits. This is a self-induced vibration, not sensitive to imbalance, where the rotor will whirl at a frequency approximately equal to that of a critical speed even though the shaft rotational speed is supercritical. This behavior is unlike a critical speed resonance where the amplitude builds up to a maximum value and decreases as the rotor speed changes. At the onset of nonsynchronous whirl, the amplitude will continually increase with speed and time. As the speed increases, the vibration levels will grow. The exciting force is not imbalance but the frictional force due to the relative motion of the splines or press fits. It takes the form of $F = K(\omega - \omega_{cr})$, where K is a constant (>0) for a given rotational speed (ω), and ω_{cr} is the critical speed. When $\omega < \omega_{cr}$ the whirl motion is damped out and the system is stable. However, when $\omega > \omega_{cr}$ the rotating damping force becomes an excitation force, adding energy to the system and causing the whirl amplitude to increase. If unrestrained, this can lead to extensive damage or destructive failures.

The power rotor system of a typical gas turbine engine which has been experiencing some nonsynchronous vibration was analyzed to determine which parameters have the greatest effect on the system stability. It will be shown both analytically and by testing that external damping at a sensitive bearing location is an effective method for controlling nonsynchronous vibrations, and the squeeze film damper is a practical answer for achieving the required damping. The squeeze film damper's design philosophy, a description of its operation, and the avoidance of instability associated with the damper itself will be presented. It will also be shown that an alternative method for removing this instability is the complete elimination of spline friction by replacing the splined joints with flexible couplings.

ANALYSIS

The phenomenon of nonsynchronous vibration has been discussed extensively in the literature, beginning with A. L. Kimball, Jr. in 1923 (1). Crandall (2) published a physical explanation of the destabilizing mechanism using a planar model of a rotor with internal and external viscous damping. The internal damping is visualized as a drag force on the orbit. When the rotation is faster than the whirl, this drag force acts to excite the rotor. He shows that the stability of the system is dependent upon a balance between the power input into the system and the energy dissipated. If the power input is greater than the power dissipated, the energy of the orbit increases and the system becomes unstable.

Gunter (3) has conducted extensive mathematical analyses for a single mass rotor on an elastic foundation to determine what factors influence the rotor speed at which nonsynchronous vibration manifests itself. He calls this the stability threshold. Among his conclusions are that stability can be improved by reducing the internal friction and by introducing external damping. He also concludes that asymmetry of bearing supports, even without the benefit of external damping, can dramatically improve the system stability.

Figure 1 shows a model of the power rotor system whose vibration signature contains a nonsynchronous component at speeds higher than the first rigid body critical speed. The mechanism for the nonsynchronous excitation in this case is the friction force developed in the two splines. In order to analytically determine the factors that influence the stability of this rotor system, it was necessary to develop a "spline element" which accurately accounts for the destabilizing effects of rotating internal friction and incorporate this into a finite element rotor analysis program. Once this was accomplished, the stability of the system was studied by calculating the system complex eigenvalues. The imaginary part of the eigenvalue determines the frequency of oscillation and the real part determines stability. Negative (positive) values of the real part indicate that the system will be stable (unstable) for that mode of vibration.

Although the friction in the spline acts as coulomb friction, it can be adequately represented using an equivalent viscous damping coefficient (4). The equations relating force to displacement and velocity for a two degree of freedom spline element with rotating viscous damping have been derived. For simplicity, only the translational degrees of freedom have been considered. The equations for the rotational degrees of freedom follow in a similar manner. The governing equations for the translations become:

$$\begin{Bmatrix} F_X \\ F_y \end{Bmatrix} = \begin{bmatrix} b & 0 \\ 0 & b \end{bmatrix} \begin{Bmatrix} \dot{X} \\ \dot{Y} \end{Bmatrix} + \begin{bmatrix} k & 0 \\ 0 & k \end{bmatrix} \begin{Bmatrix} X \\ Y \end{Bmatrix} + \begin{bmatrix} 0 & b\omega \\ -b\omega & 0 \end{bmatrix} \begin{Bmatrix} X \\ Y \end{Bmatrix}$$

$$[B] \qquad [K] \qquad [K_r]$$

Where:

F_X, F_y	forces in the two mutually perpendicular directions, x and y respectively
X, Y	displacements of the two coupling parts relative to each other in the x and y directions
$\dot{X}, \dot{Y}$	relative velocities in these two directions
b	spline equivalent viscous damping coefficient
k	spline stiffness
ω	system rotational speed
B	spline damping matrix
K	spline stiffness matrix
K_r	spline rotating friction matrix

The skew - symmetric terms in the $[K_r]$ matrix are those which may cause the system to become unstable, depending on their magnitude. Thus, the system will tend to instability for high values of the damping coefficient and high rotor speeds, providing there is some relative motion in the spline.

The major difficulty in accurately modeling the system is that the spline stiffness and friction force vary with the transmitted torque. Because these values are difficult to predict, the analysis takes the form of a parametric study to determine the relative contribution of the variables to the system stability. This provides information as to the design changes which may be beneficial and the direction in which further testing should proceed. The variables to be investigated are spline friction, bearing damping, and support asymmetry.

The nominal values of the parameters are shown in Figure 1. Figure 2 shows the mode shape corresponding to the only critical speed in the rotor's running range of 0 - 22,000 rpm. The mode shape depicts the shafts moving as rigid bodies, essentially hinged at the two splines. Most of the strain energy is in the No. 2 bearing but there is substantial relative motion at the first spline and some relative motion at the second spline. The friction forces due to these motions will overcome the minimal damping at the bearing locations and induce a nonsynchronous vibration when the rotor speed is greater than the first critical speed for forward precession. The frequency of this vibration as a function of rotor speed is plotted in Figure 3. The speed dependence of the natural frequency is due to gyroscopic effects and the circled points denote the critical speeds for forward and reverse precession. In

this analysis, the mode for reverse precession was found to be stable for all cases. The result is in agreement with previous analytical work which has determined that internal damping will act to stabilize this mode (2, 5).

A stability map of the system (Figure 4) can be obtained by solving for the damped natural frequencies at various rotor speeds (ω) and plotting ω vs. the system logarithmic decrement. The logarithmic decrement is defined as δ = ln (X1/X2) where X1 and X2 are two successive peak amplitudes of deflection. It is a measure of the rate at which the vibration amplitude is decaying or growing with time and can be given by $\delta = -2\ \mathrm{Re}(\lambda)/\mathrm{Im}(\lambda)$, where Re(λ) is the real part of the eigenvalue and Im(λ) is the imaginary part. The system is unstable for negative values of the logarithmic decrement. As is evident from Figure 4, the rotor system with minimal external damping becomes unstable at its critical speed for forward precession. (ω s= ω cr=9750 rpm). The rotor will continue to whirl at a frequency approximately equal to ω cr even though the rotor speed increases.

The behavior of the system at various rotor speeds is further explained by looking at the whirl orbits obtained from a transient analysis (Figure 5). The forcing function was taken as a small imbalance with a frequency equal to the rotor speed. For speeds below the critical speed, the imbalance causes the orbit to spiral out initially, but it recovers into a stable, synchronous motion. At the stability threshold, the motion is synchronous but unstable. For speeds above the critical speed, a component of nonsynchronous precession appears due to the friction in the splines. As time progresses the nonsynchronous component overpowers the synchronous motion and the orbit diverges.

It has been suggested in the literature that a reduction in spline friction can delay the onset of nonsynchronous vibration. This was analyzed by setting the friction in the second spline to zero and varying the friction in the first spline. Figure 6 plots the system logarithmic decrement against the spline angular damping coefficient for various rotor speeds. It is observed that reducing spline friction will improve the system stability but, in the absence of external damping, the friction must be all but eliminated to ensure stability throughout the operating range.

Anisotropic supports may also help stabilize a system. The stiffnesses of the No. 1 and No. 2 bearings were altered in one plane and left unchanged in the other orthogonal plane to determine the effect of support asymmetry on the stability of this system. Figure 7 shows the dependence of the stability threshold on the support flexibility ratio. Increasing the support stiffness in one direction will give a significant improvement in the stability threshold but will also introduce a system resonance in the range of steady operation. This is unacceptable and the only option is to reduce the support stiffness. The stability improvement for this condition is not dramatic, requiring supports which are very asymmetric to guarantee stability throughout the running range. This can cause large excursions due to imbalance.

A very effective way to increase the system stability threshold is to add external damping to the system. The easiest way to achieve this is to introduce damping at the bearing locations. For the mode shape of interest (Fig. 2) most of the motion is in the No. 2 bearing. This is a prime location to introduce damping, as the motion allows for greater energy dissipation. Figure 8 shows the improvement in the stability threshold due to external damping at this bearing.

CONCLUSIONS BASED ON ANALYSIS

The conclusions of the parametric analysis of spline - induced nonsynchronous vibration for this rotor system are as follows:

1. Asymmetric supports will help stabilize the system, but the asymmetry must be great to completely eliminate nonsynchronous precession. Therefore, the degree of asymmetry required to stabilize this system is impractical.

2. Reduction of spline friction will improve the stability, but without external damping, the spline friction must be all eliminated to ensure stability at all rotor speeds.

3. Introduction of external damping in the proper bearing location will dramatically improve the system stability characteristics and provide relief from nonsynchronous vibration.

TEST HISTORY

Instability Verification

A nonsynchronous excitation of the first whirl mode has frequently occurred during engine operation. The response, as measured by transducers on the engine casing, sometimes would be above the established acceptable limits. A Campbell diagram constructed from the response of a typical transduer from one of these engines is shown in Figure 9. The plot shows that the synchronous excitation of the whirl at the running speed of 9000 rpm was negligible, indicative of good balance. As the running speed increased the vibration remained low until approximately 11,000 rpm where a nonsynchronous excitation of the whirl was initiated. Once initiated the instability remained throughout the rest of the operating range up to 22,000 rpm. The precise frequency of this whirl varied from engine to engine between 150 hz and 195 hz. This difference may have been due to variation in geometry and load sharing of the number 1 and 2 bearings. The speed at which the instability was initiated also varied from engine to engine.

Instability Attenuation

During the initial development of this system the two splines were unlubricated. The introduction of lubrication into the splines substantially improved the system stability but, as indicated in the analysis, it did not eliminate thr problem for all engines. The mechanism of spline friction exciting this whirl was understood, however it was unclear why some engines were strongly excited while others ran smoothly. Balance and dimensional checks of the rotating hardware components did not reveal any consistent explanation for the variation in response.

A rig which closely simulates this system was used for some controlled studies. The rig allowed a parallel offset of the numbers 3 and 4 bearings with respect to numbers 1 and 2 bearings to be controlled, creating a misalignment angle in the two splines. A displacement probe transducer was used to measure the deflection of the center of the power shaft. The rig was run with different misalignment settings

from 0 degrees to 1 degree to determine the effect on the instability. Figure 10 shows Campbell diagrams generated by the response of this rig under three of the different misalignment conditions. The results indicated that the instability was effectively attenuated with misalignment angles greater than an eighth of a degree.

In the engine, the direct measurement of misalignment of the rotor system was not practical. In order to obtain some idea of the alignment condition of the rotor system in engines, a special tool was devised which quickly measured the radial and angular offsets due to the principal stackup items between the number 1 and 2 bearings and the number 3 bearing. These measurements were then used to calculate both the magnitude and orientation of misalignment angle in the two splines. This alignment check was conducted during the assembly of approximately sixty engines. Figure 11 shows polar charts of these results. The magnitude of the misalignment is represented radially outward while the orientation angle is represented circumferentially. The engines which produced a high nonsynchronous vibration are distinguished on the plot from the engines which ran smoothly.

The initial observation from these results was that there was no correlation between the magnitude of misalignment based on these measurements and the level of nonsynchronous vibration. However scrutiny of the discrepant engines' alignment data revealed them to be clustered between -30 degrees and +30 degrees orientation angle and a magnitude greater than 0.09 degrees misalignment angle.

This clustering of points is believed to be indicative of a shift in the alignment of this system between the measured state, before final assembly, and the assembled running state. This shift brings the points clustered in the critical zone down to near the perfect alignment area. While the bearing supports are essentially axi-symmetric, both the temperature distribution and the engine casing stiffness in this area are not uniform in the vertical plane. This may account for a static shift in the alignment condition of the splines.

The use of these measurements and the previously defined critical zone as a screening procedure for engines being assembled virtually eliminated the number of engines experiencing excessive nonsynchronous vibration levels at test. The residual misalignment left in the splines was always held to within one half degree to prevent spline wear or the introduction of high misalignment forces into the system.

The conclusion drawn from these results was that a small misalignment of a splined system significantly improved its stability. One explanation for this behavior is that the misalignment imposes a limit on the whirl orbit by creating an effective spline stiffness asymmetry.

The use of this controlled alignment procedure consistently reduced the amplitude of the instability to within acceptable limits however it did not eliminate it.

INSTABILITY ELIMINATION (FLEXIBLE COUPLINGS/SQUEEZE FILM DAMPERS)

Two possible approaches aimed at the complete elimination of the instability were indicated by the analysis. One is to replace the two splines with dry flexible couplings having no sliding friction surfaces to excite the instability. The second is to add external damping at the appropriate bearings in order to counteract the internal damping generated by the splines.

The first approach using a flexible coupling has been tested in the rig described earlier. The whirl mode of the system with the flexible couplings is essentially unchanged from the splined system. Figure 12 shows a Campbell diagram generated by the response from a displacement probe sensing the deflection of the shaft between the couplings. The synchronous response of the whirl mode is clearly seen to be excited but no nonsynchronous excitation is apparent. This result was repeatable for all misalignment settings. An additional benefit of this type of coupling is that no lubrication is required, since there is no sliding involved in the flexing joints. Due to other considerations some operating conditions may be too severe for this type of couplings use.

In order to address the second approach squeeze film dampers have been designed for the number 1 and 2 bearing locations. The analysis indicated that a damper located at only the number 2 bearing is sufficient. Dampers at both locations are being employed for nondynamic design considerations. A discussion of the design of squeeze film dampers follows.

SQUEEZE FILM DAMPER (ANALYSIS AND OPERATION)

The squeeze film damper is a practical answer to the external damping required by analysis. Its purpose is to reduce to acceptable limits the lateral amplitudes of shaft - rotor systems operating at or above a critical speed and/or to cushion the loads on rolling contact bearings when such loads are excessive. For rigid body whirl modes, with large excursions at one or more bearing locations, squeeze film dampers are placed at these bearings for effective vibration attenuation. The shaft's precessional motion associated with these whirl modes may be either synchronous or nonsynchronous. For shaft bending modes that possess little motion at a bearing location, a damper at that location is ineffective; therefore, a more strategic location must be determined or a rotor redesign considered.

A squeeze film damper consists of a cylindrical inner member and a hollowed outer member separated by a thin fluid film, usually oil. Figure 13 shows a typical squeeze film damper. During lateral motion of the inner member, which is the outer race of the bearing, oil is squeezed out from the cavity between the two members. This squeezing action produce fluid forces, which for a properly designed damper will dissipate energy and aid in the reduction of excessive amplitudes and/or bearing forces.

The squeeze film damper considered in this report is one whose inner member is prevented from rotating by an antirotation device and whose axial length, L, (or series of axial lengths) is sufficiently short, making the effect of circumferential flow negligible. The pressure generated by the squeezing action is assumed to be sufficiently high, allowing for the consideration of only the positive portion of the pressure wave, which is conservative for low values of the eccentricity, ϵ .

Reynold's equation for short damper analysis was simplified by assuming the following: the radial clearance, C, and displacements are small compared to the radius, R, of the damper; the viscosity, μ, is constant in the axial and circumferential directions; the film thickness is constant in the axial direction; and the pressure profile is parabolic in the axial direction. Integration of the simplified Reynold's equation was accomplished in closed form, yielding the pressure profile in the circumferential direction. Integration of the positive portion of the pressure

profile gave the load carrying capacity in the component directions, radial and tangential. The radial and tangential fluid forces on the inner member are given by:

$$\begin{bmatrix} W_R \\ W_T \end{bmatrix} = \mu R \left(\frac{L}{C}\right)^3 C \begin{bmatrix} J_{11} & J_{12} \\ J_{12} & J_{22} \end{bmatrix} \begin{Bmatrix} \dot{\varepsilon} \\ \varepsilon\dot{\phi} \end{Bmatrix}$$

WHERE $$J_{11} = \int_{\theta_1}^{\theta_2} \frac{\cos^2\theta \, d\theta}{(1+\varepsilon\cos\theta)^3}$$

$$J_{12} = \int_{\theta_1}^{\theta_2} \frac{\sin\theta\cos\theta \, d\theta}{(1+\varepsilon\cos\theta)^3}$$

$$J_{22} = \int_{\theta_1}^{\theta_2} \frac{\sin^2\theta \, d\theta}{(1+\varepsilon\cos\theta)^3}$$

AND $$\theta_1 = \tan^{-1}\left\{\frac{\dot{\varepsilon}}{\varepsilon\dot{\phi}}\right\}$$

$$\theta_2 = \theta_1 + \pi$$

The expressions $\dot{\varepsilon}$ and $\varepsilon\dot{\phi}$ are the dimensionless instantaneous velocities of the inner member's center in the radial and tangential directions, respectively.

If $\dot{\varepsilon}$ is set equal to zero, ε constant, and the precessional speed, $\dot{\phi}$, is set equal to the rotative speed ω , the special case of steady synchronous motion, commonly found in actual operation, is the result. The J factors are no longer time dependent, but reduce to simple, yet highly nonlinear algebraic expressions. The equation governing the dimensionless response for rigid body whirl for a rotor of effective mass, m, and unbalance distance, δ , is determined by vectorally equating the fluid forces to the rotor's inertia force. Figure 14 graphically depicts the response, ε , versus the dimensionless speed

$$\frac{m\omega}{\mu R}\left(\frac{C}{L}\right)^3 = \frac{\omega}{Q}$$

for various values of the dimensionless unbalance δ/C.

Squeeze film damper properties described above are also applicable to flexible rotor systems. Forced response computer programs based on both the transfer matrix approach and finite element approach have been developed for multidampers and multilevels. Before proceeding with specific applications, consider the general motion case.

For the general rigid body motion case, no assumptions concerning kinematics were made; rather, the radial and tangential components of the $m\bar{a}$ force in its full form were equated to the fluid forces, resulting in two time dependent equations, which were programmed with appropriate initial conditions and then solved. Polar

plots of ε versus the precessional angle were generated, representing the dimensionless motion of the center of the inner member during both steady-state and transient response. Plots were made for rotative speeds, ω, of 160, 400, 800, 1600 and 4000, while Q values of .4, 4, 40 and 400 were used. For each combination of ω and Q various values of the dimensionless unbalance δ/C were tried, which, during solutions were instantaneously increased to new values, yielding the ensuing transient response. Only a select few of these plots are shown in Figure 15, which is summarized as follows:

FIGURE	ω rad/sec	Q rad/sec	ω/Q	δ/C	COMMENT
15a	1600	400	4	.5 - 1.5	STABLE
15b	1600	40	40	.5 - .6	SOMEWHAT UNSTABLE
15c	1600	4	400	.5 - .55	UNSTABLE
15d	4000	.4	1000	.1 - .15	UNSTABLE

The ratio ω/Q is the main ingredient for determining damper stability. Low values of this ratio yielded stable and "safe" operation ($\varepsilon < .9$) for wide ranges of unbalance; high values of ω/Q produced unstable and often "critical" operation ($\varepsilon > .9$), even for small changes in unbalance; and intermediate values gave both stable and unstable results in the safe and critical ranges, depending on the magnitudes of the unbalances used and their increments.

Consideration of these computer solutions together with the plot, Figure 14, clarified the operational limits of the squeeze film damper described. These limits are summarized in Figure 16, which is a plot of dimensionless unbalance vs. dimensionless speed ω/Q. It defines those combinations of design parameters under which damper instability and/or critical operation is predicted.

Figure 17 shows a comparison of the predicted steady state synchronous response of the system with standard bearings versus squeeze film bearings at the numbers 1 and 2 locations. Based on the stability analysis described earlier the damping obtained from these squeeze films is well above the level found to be needed to suppress the nonsynchronous whirl. In order to prevent damper instability, the above damper analysis was used along with the steady state response analysis to size the damper dimensions. Testing of this rotor system with squeeze film dampers is pending. This analytical process has been used to design squeeze film dampers for another splined rotor system which experienced a similar subsynchronous excitation of a whirl mode. Subsequent testing of this rotor system confirmed the analytical results.

SQUEEZE FILM DAMPER DESIGN PHILOSOPHY

The design philosophy used at Lycoming for squeeze film dampers depends upon whether or not the bearing being damped carries a unidirectional thrust load. Figure 13 depicts a ball bearing/squeeze film damper configuration which carries a thrust directed to the left for all shaft speeds. For this condition the reaction takes place at the hard faced surface, which also acts as a seal against oil loss. Oil is introduced at the outer diameter of the bearing and flows through the annular

clearance provided between the bearing outer race and the liner inner diameter. An upstream orifice is sized to prevent pressurization of the damper while maintaining a copious supply of oil to replace that which is lost. The circumferential groove acts as an oil reservoir during the squeezing action; i.e., the rotating positive pressure profile generates flow into the reservoir while the virtual negative pressure profile, 180° away, causes the flow from the reservoir back into the annular clearance. Of course, there is still a net flow of oil out, as shown. For maximum load carrying capacity and minimum oil loss, the volume of the reservoir need not be greater than the flow into it, and it should be placed as close to the bearing's extremity as is practical.

If a squeeze film damper is required at a bearing that carries a bidirectional thrust load or none at all, sealing does not take place, rather oil flows out both ends of the damper (Figure 18). In this configuration, oil is introduced at the center of the damper into a circumferential groove and flows along the annular clearance and into the reservoirs, which serve the same purpose as the single reservoir in the previous configuration. Other parameters remaining unchanged, the flow requirement is doubled, and since the load carrying capacity varies as the cube of the length, the capacity for both "halves" is one-fourth. In order for the split configuration to carry the same load as the unsplit one, the length of each half must be made to 80% of the uninterrupted length. For certain applications the total length requirement may not be achievable by using a bearing of usual proportions, and in these cases bearing manufacturers can supply longer outer races.

CONCLUSIONS

Analysis and testing of the power rotor system of a typical gas turbine engine has resulted in certain conclusions regarding spline induced subsynchronous vibrations.

1. Asymmetric supports tend to stabilize the system, but the degree of asymmetry required is impractical, and other vibratory problems may be created.

2. Reduction of spline friction by lubrication did not consistently control the instability, but the use of flexible couplings, which eliminates the internal friction, is a viable solution.

3. Small spline misalignment in this system significantly improved the stability.

4. Introduction of external damping by employing a properly designed squeeze film damper at a sensitive bearing location eliminates the instability.

5. The dimensionless speed number (ω/Q), which reflects the squeeze film damper's geometry as well as speed, should be selected to avoid the damper's threshold of instability.

REFERENCES

1. Kimball, A. L., Jr.: Internal Friction Theory of Shaft Whirling. Phys. Rev. (2) 21, 703 (1923).

2. Crandall, S. H.: Physical Explanations of The Destabilizing Effect of Damping in Rotating Parts. NASA CP2133, May 1980, pp. 369-382

3. Gunter, E. J., Jr.: Dynamic Stability of Rotor - Bearing Systems. NASA SP-113, Office of Technology Utilization, U. S. Gov. Printing Office, 1966.

4. Marmol, R. A.; Smalley, A. J.; and Tecza, J. A.: Spline Coupling Induced Nonsynchronous Rotor Vibrations. ASME Paper No. 79 - DET - 60.

5. Bucciarelli, L. L.: On the Instability of Rotating Shafts Due to Internal Damping. Journal of Applied Mechanics, Trans ASME, vol. 49,1982, p. 425.

6. Foote, W. R.; Poritsky, H.; and Slade, J. J., Jr.: Critical Speeds of a Rotor With Unequal Shaft Flexibilities, Mounted in Bearings of Unequal Flexibility. Journal of Applied Mechanics, Trans ASME, vol. 65,1943, p. A77.

7. Crandall, S. H. and Brosens, P. J.: On the Stability of Rotation of a Rotor with Rotationally Unsymmetric Inertia and Stiffness Properties. Journal of Applied Mechanics, Trans ASME, vol. 83,1961, p. 567.

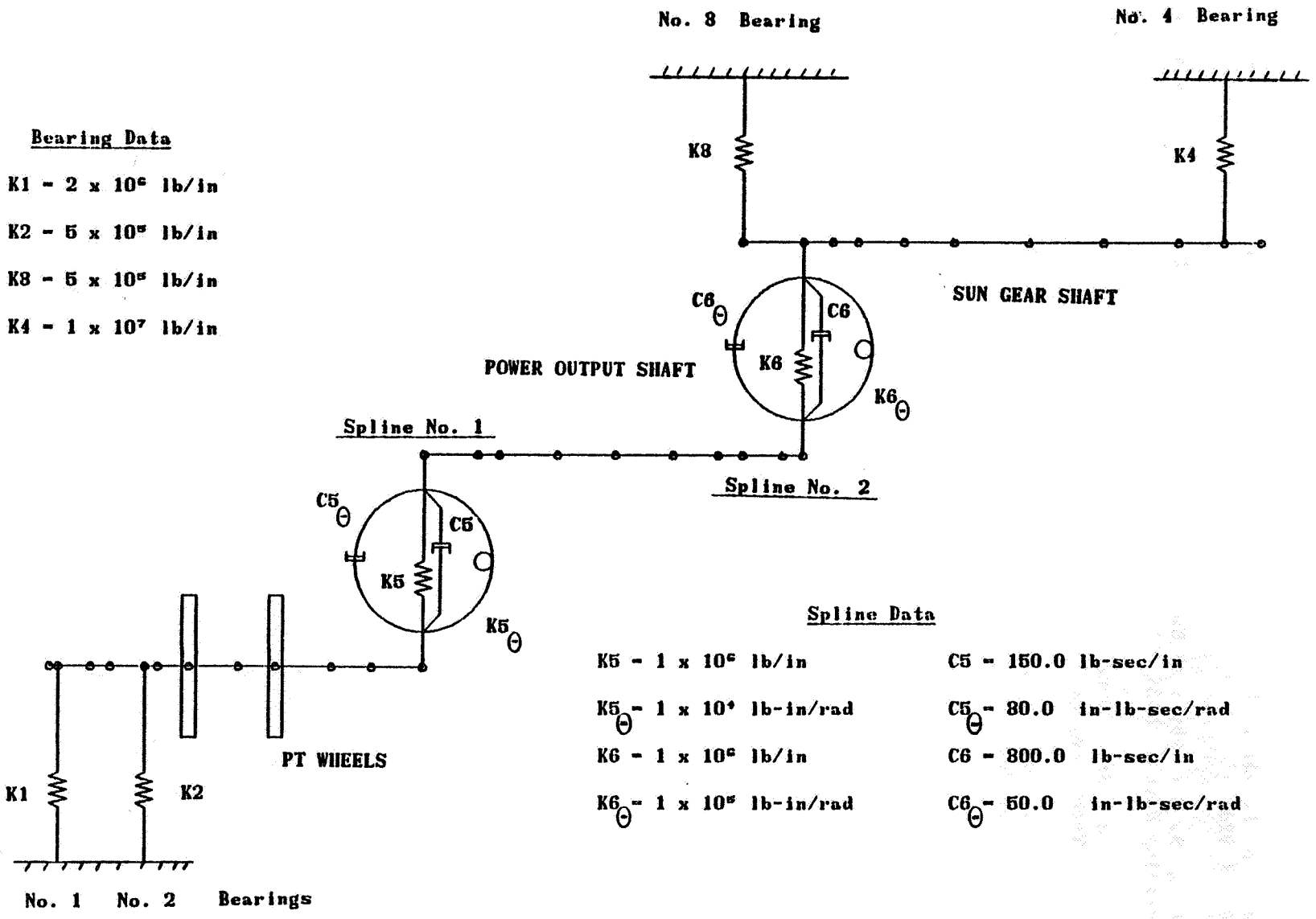

Figure 1. - Model of power turbine system with spline internal damping.

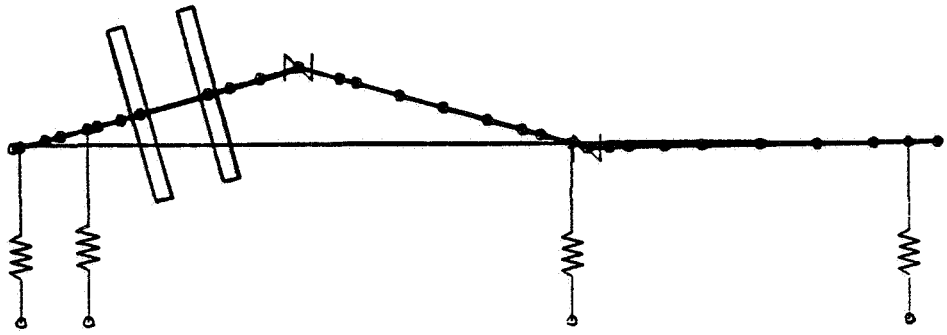

FREQUENCY - 162 Hz - 9750 CPM

Figure 2. - Power turbine whirl mode.

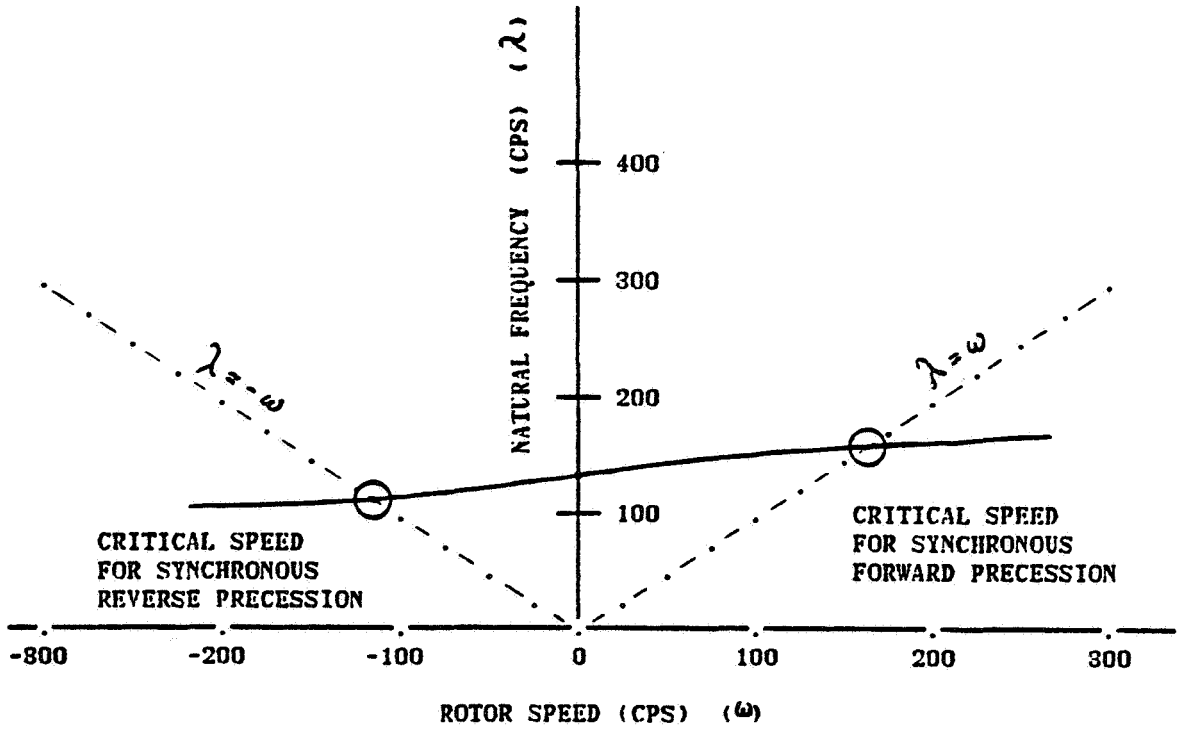

Figure 3. - Effect of rotor speed on natural frequency.

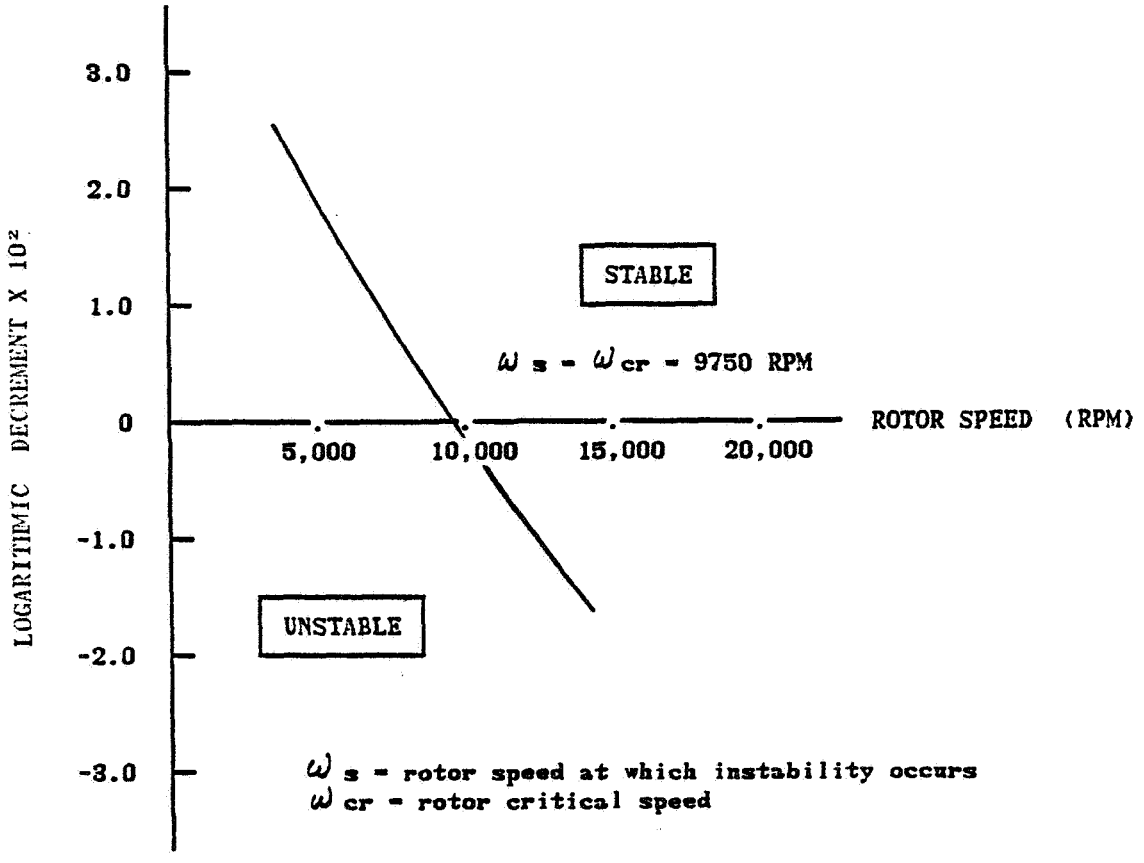

Figure 4. - Stability analysis for turbine system with no external damping (nominal case).

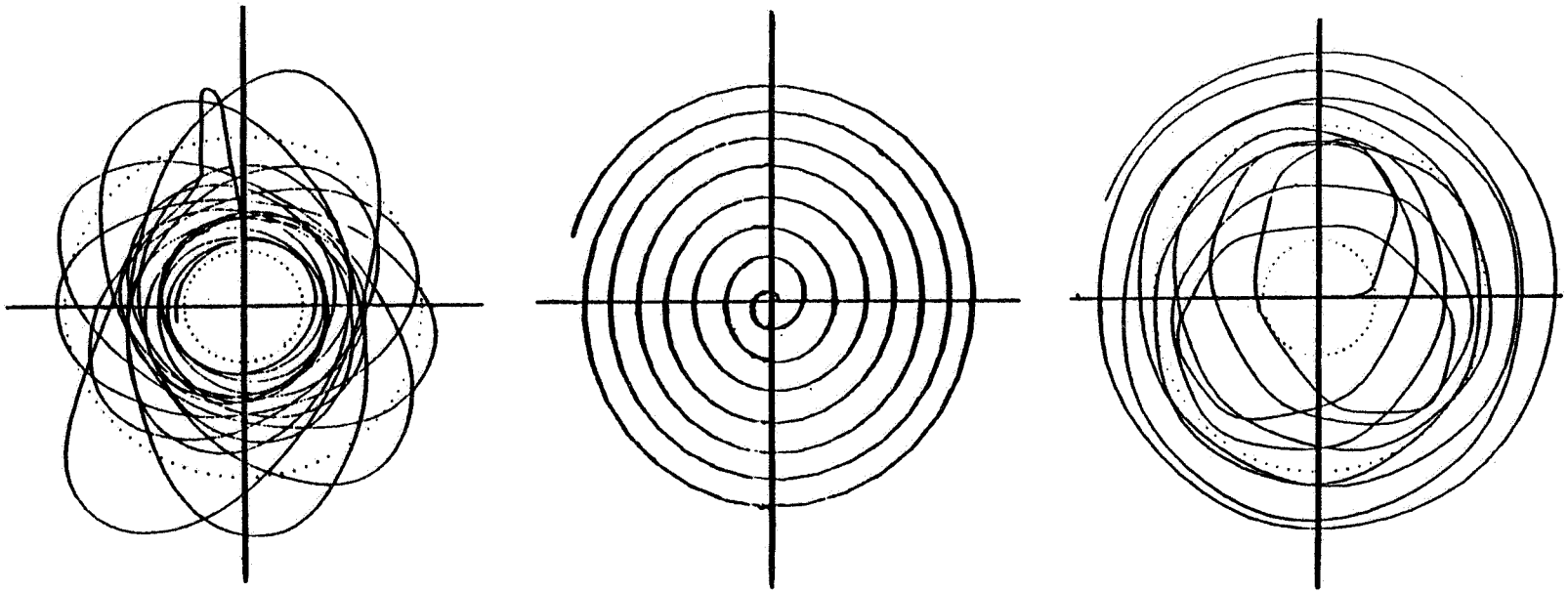

ROTOR SPEED - 5,000 RPM

$\omega < \omega_{cr}$

ROTOR SPEED - 9,760 RPM

$\omega = \omega_{cr}$

ROTOR SPEED - 20,000 RPM

$\omega > \omega_{cr}$

ω_{cr} - ROTOR FIRST CRITICAL SPEED - 9,760 RPM
ω - ROTOR SPEED (RPM)

Figure 5. - Whirl orbits for power turbine system at various rotor speeds (response to imbalance).

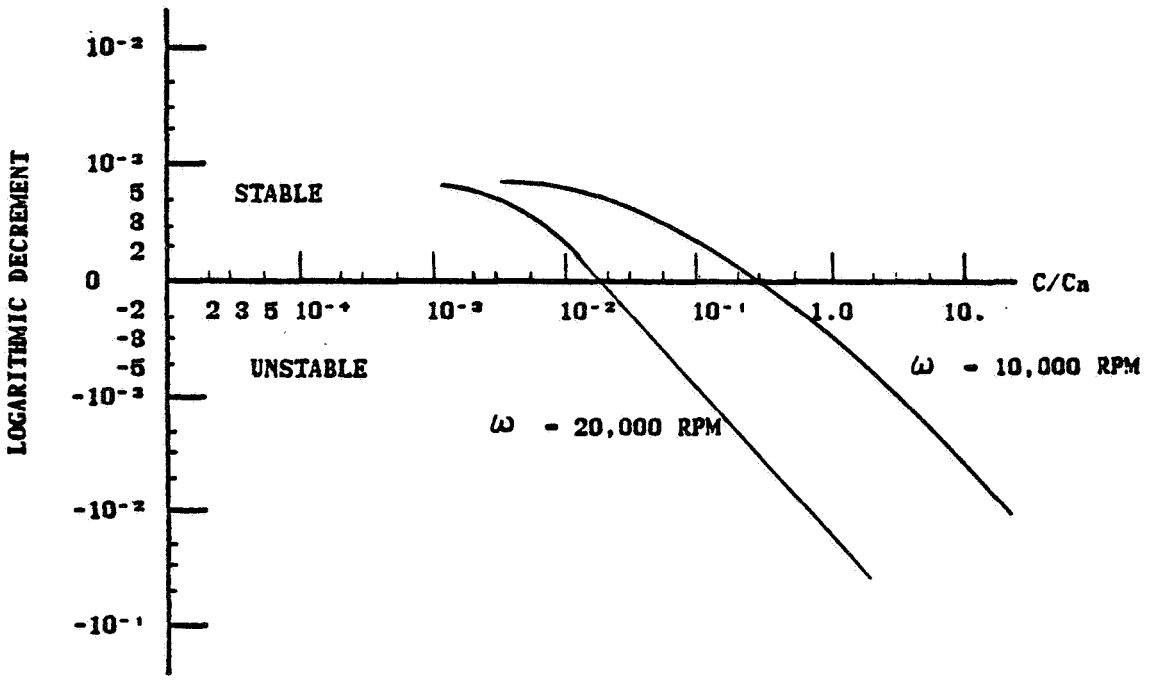

$$\frac{C}{Cn} = \frac{\text{Angular Damping Coefficient in Spline No. 1}}{\text{Nominal Value of Angular Damping Coefficient}}$$

ω - Rotor Speed

Lightly Damped Supports

Figure 6. - Effect of spline angular damping on system stability. Lightly damped supports.

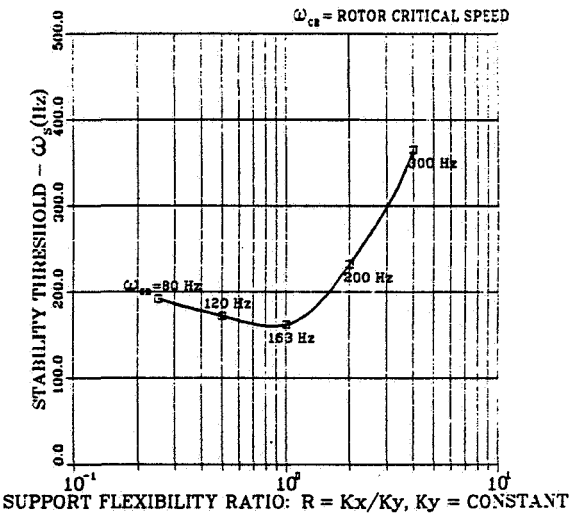

Figure 7. - Effect of foundation asymmetry on system stability threshold. Undamped supports.

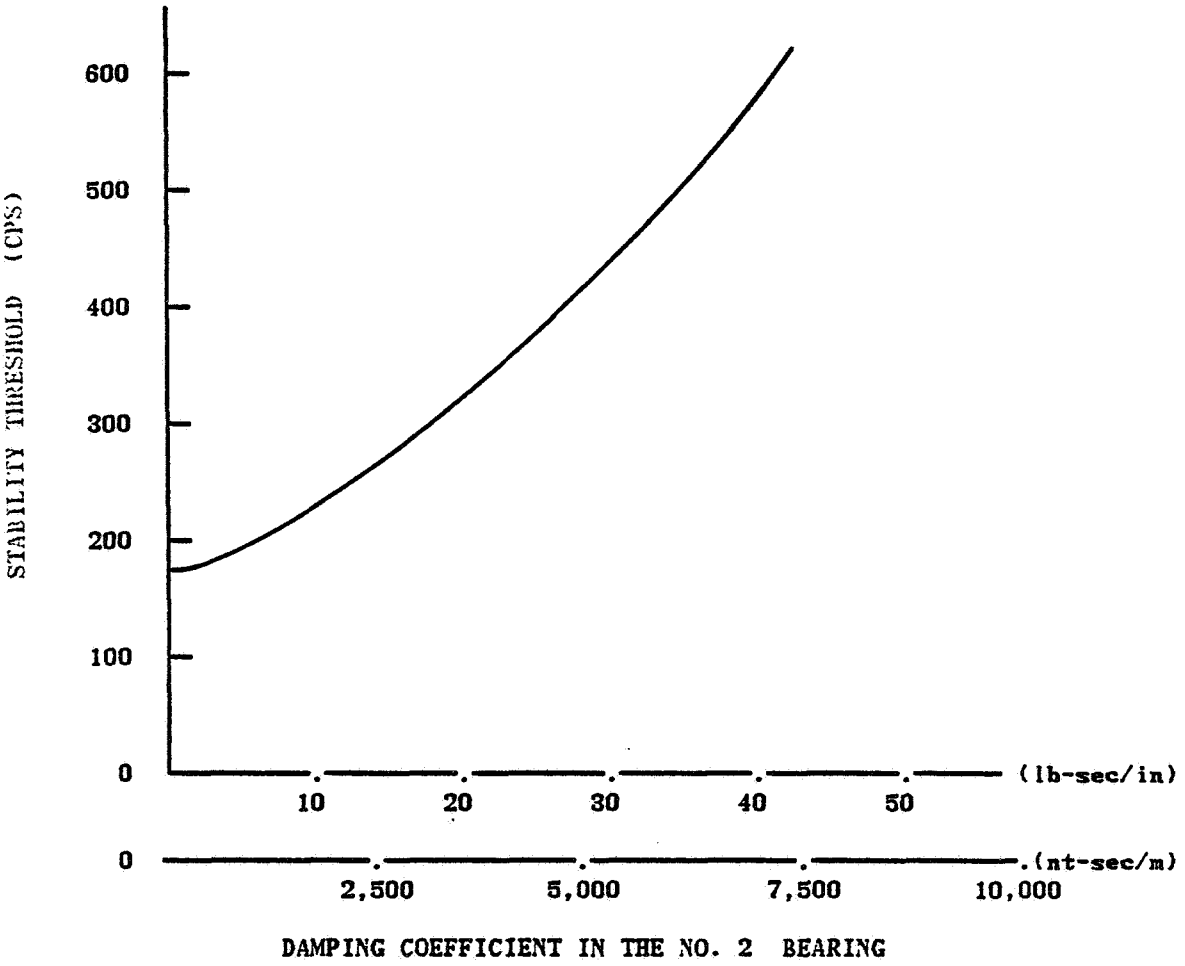

Figure 8. - Effect of damping in no. 2 bearing on system stability threshold.

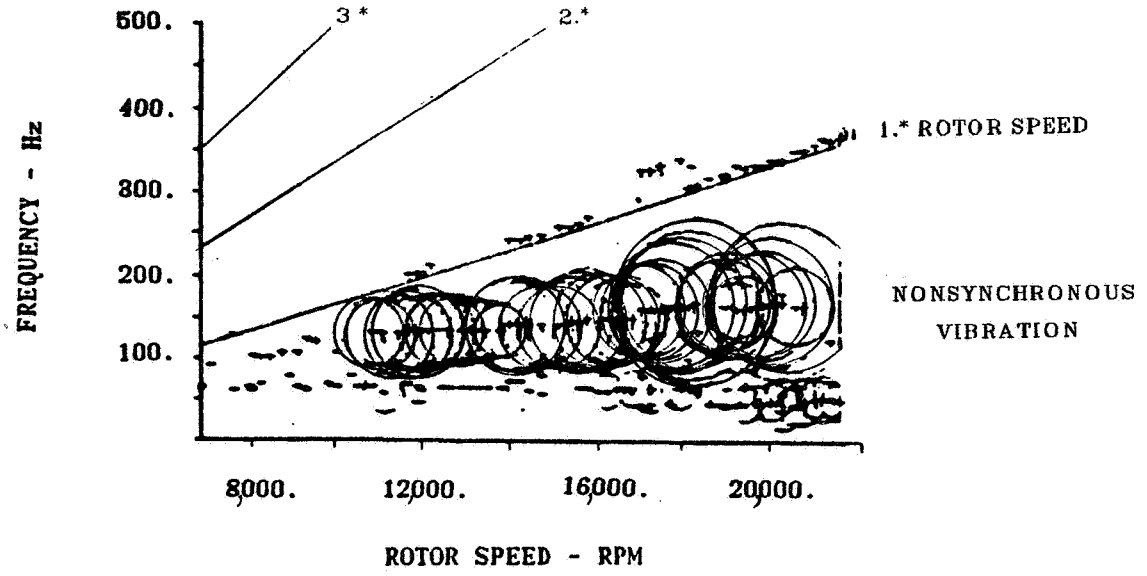

Figure 9. - Response from transducer mounted on engine casing.

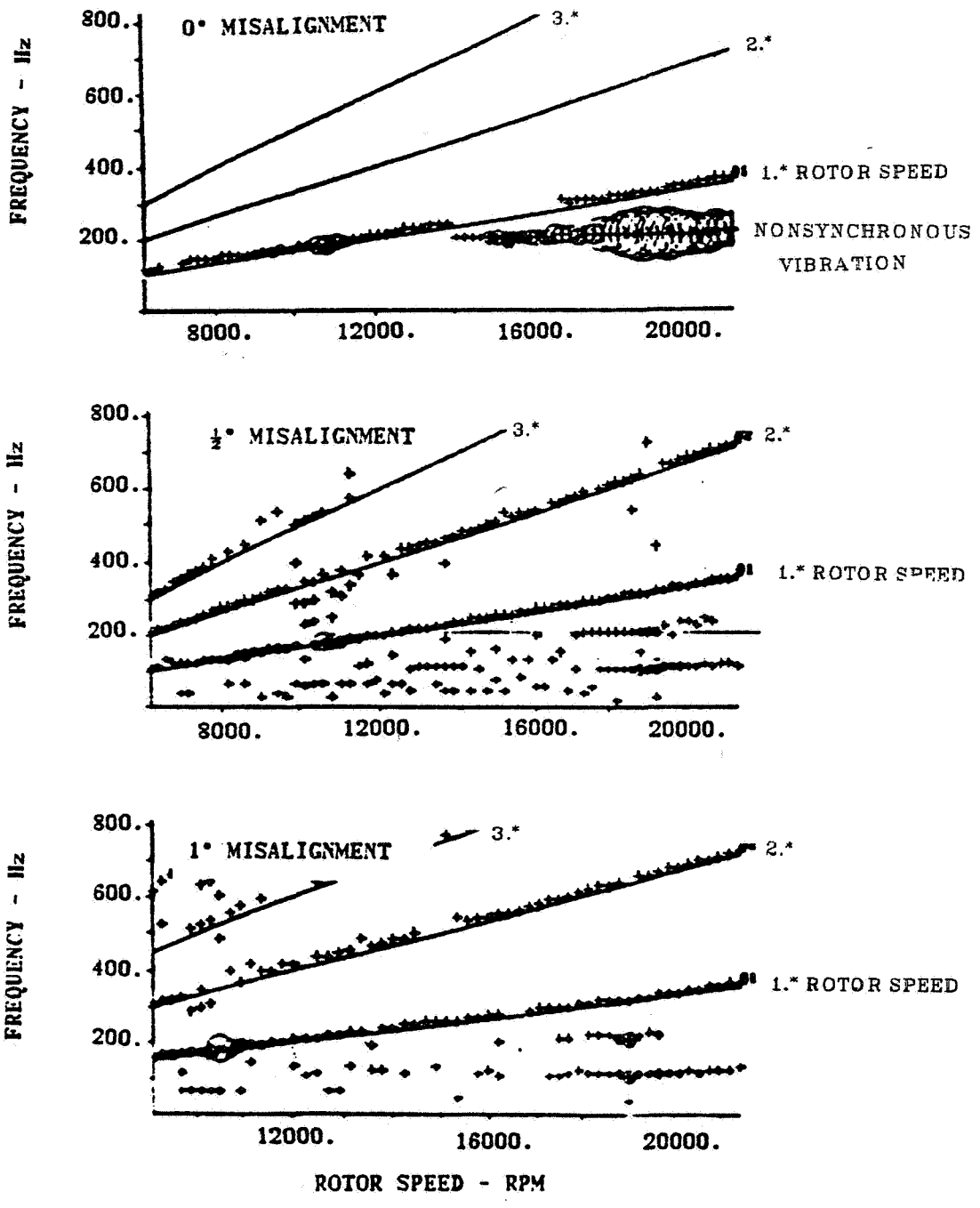

Figure 10. - Response of power shaft center from displacement probe rig with standard rotor system.

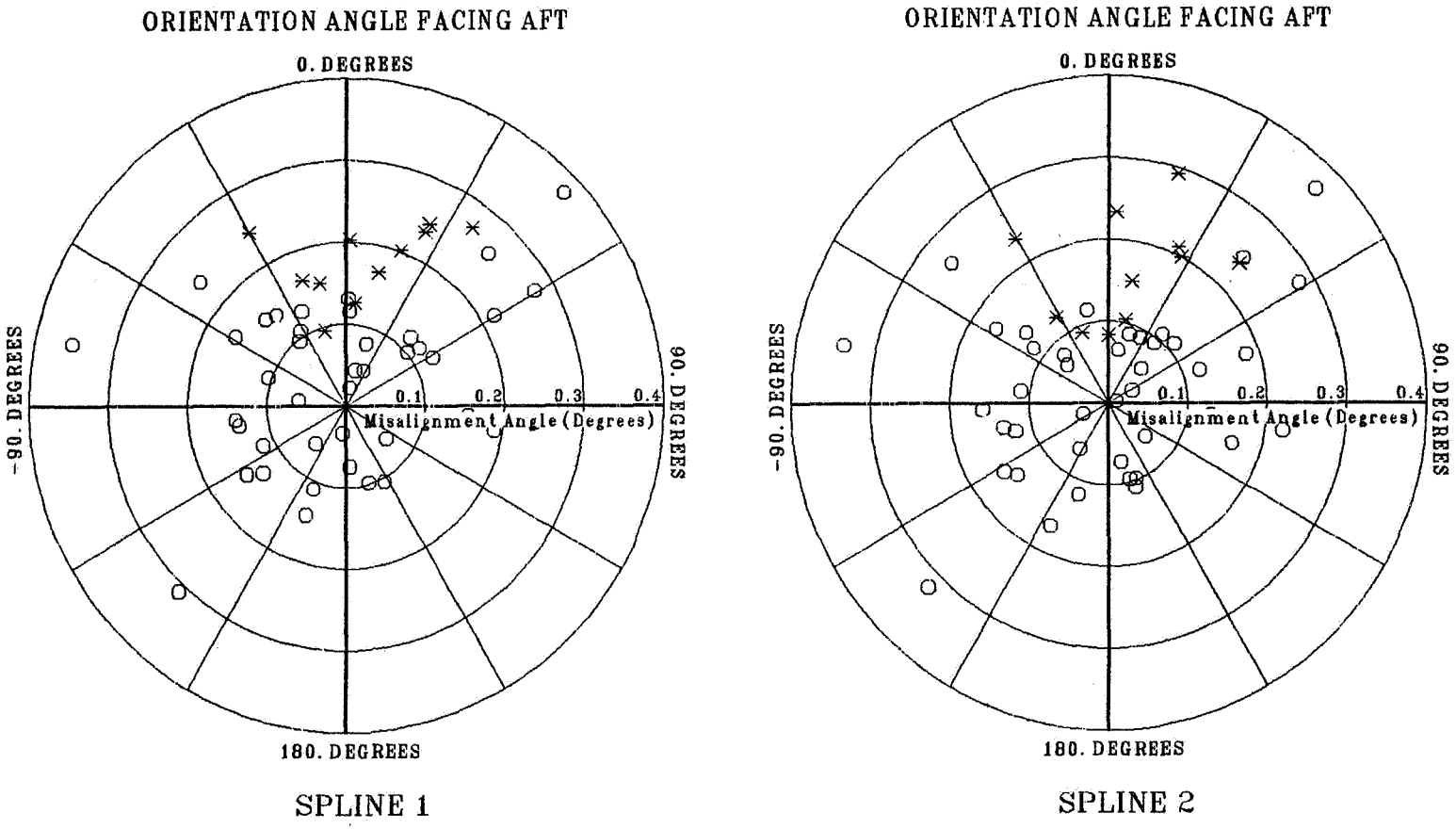

Figure 11. - Power rotor system spline alignment based on measurements of principal pilots.

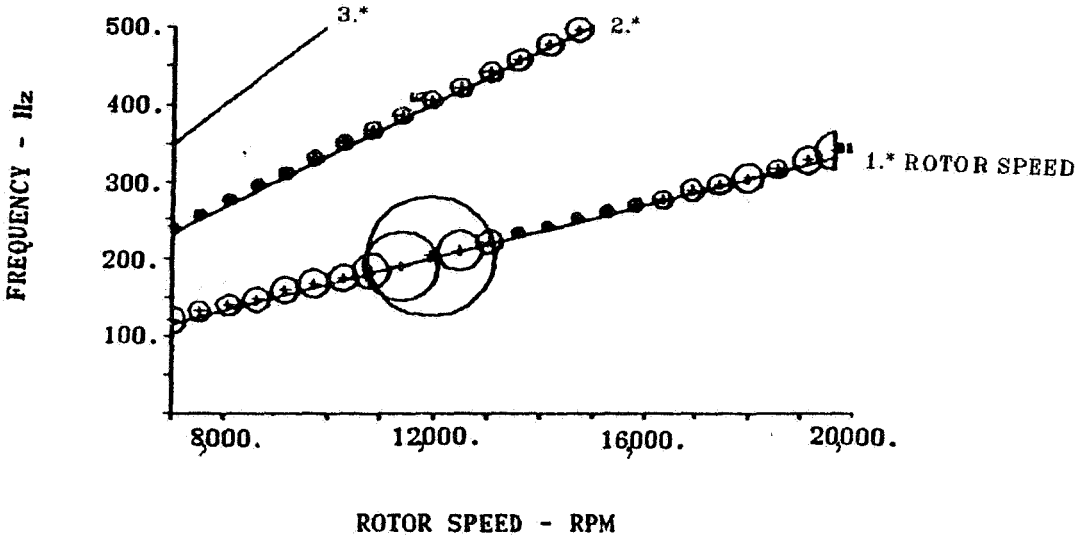

Figure 12. - Response of power shaft center from displacement probe. Rig with flexible coupling power shaft.

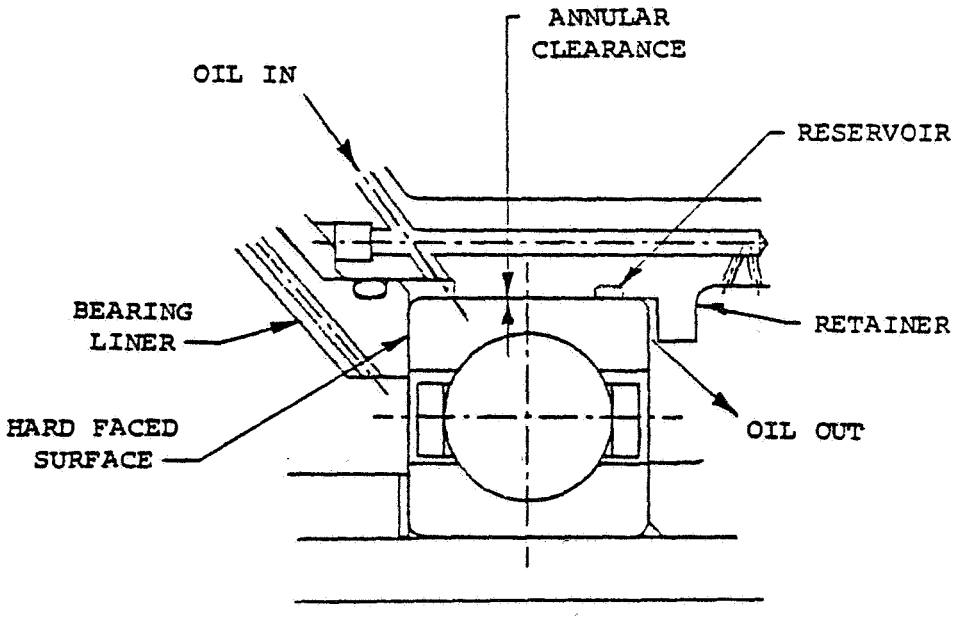

Figure 13. - Typical squeeze film damper.

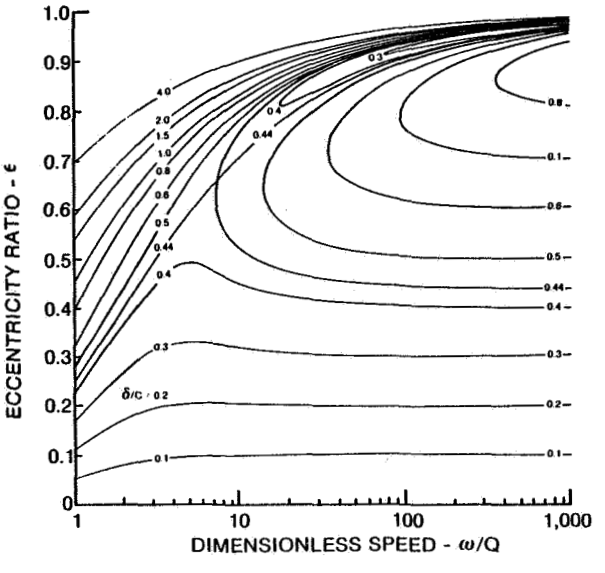

Figure 14. - Dimensionless steady state response of a squeeze film damper.

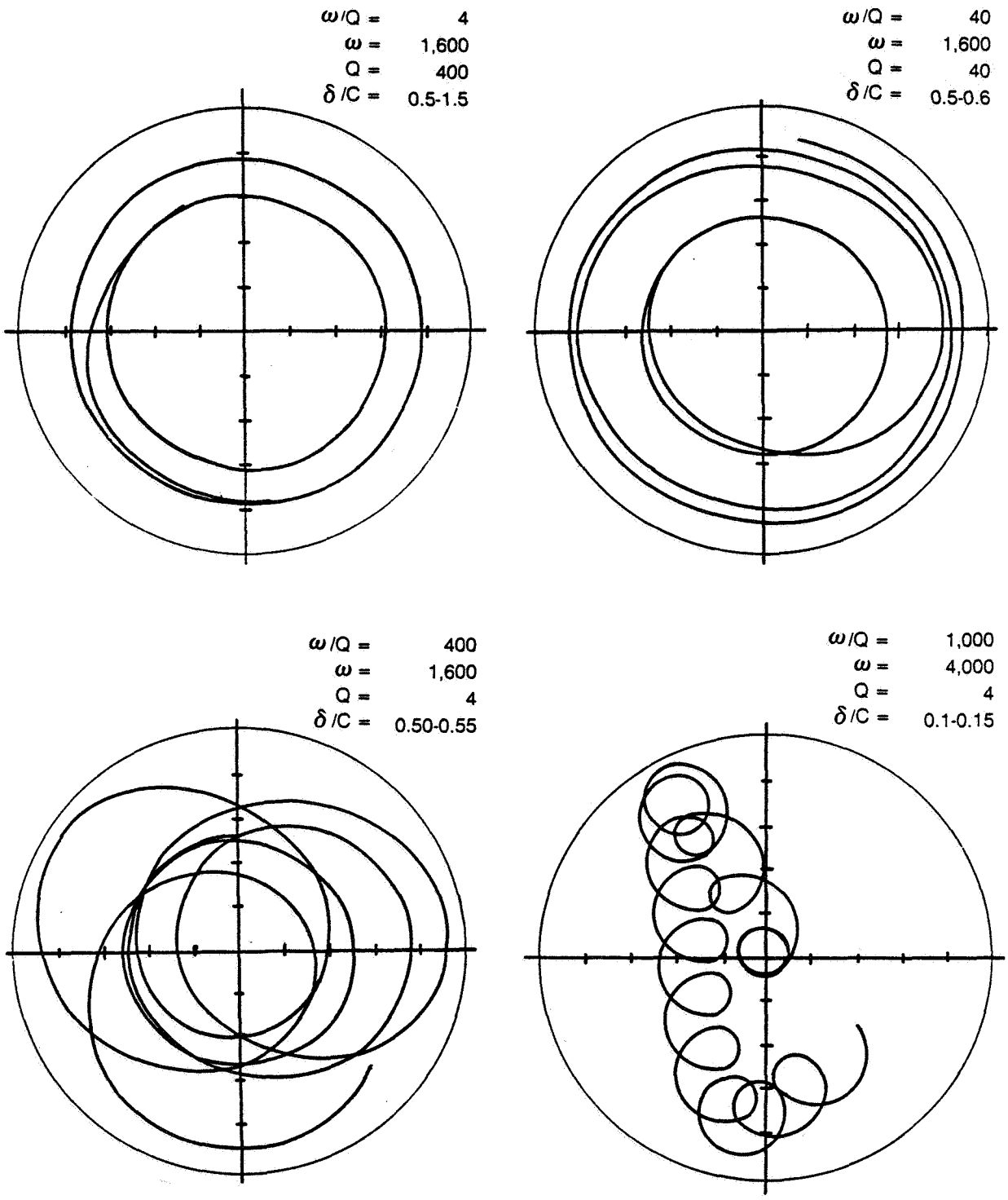

Figure 15. - Transient responses of a squeeze film damper.

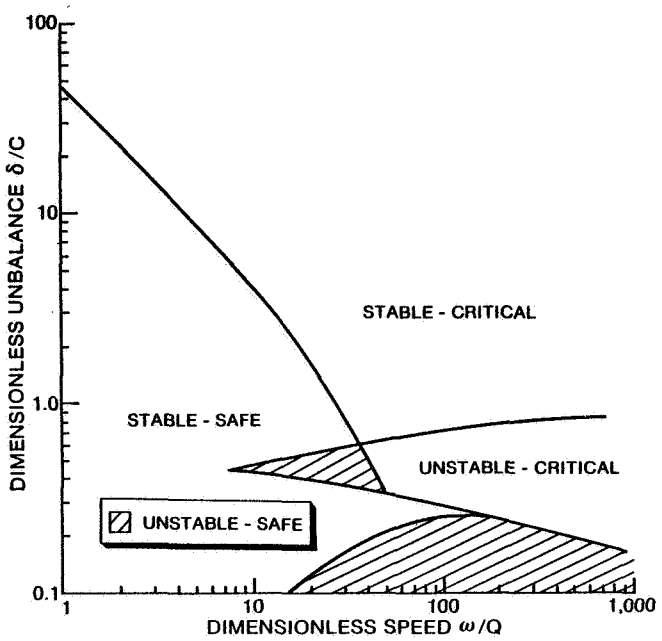

Figure 16. - Operational limits of a squeeze film damper.

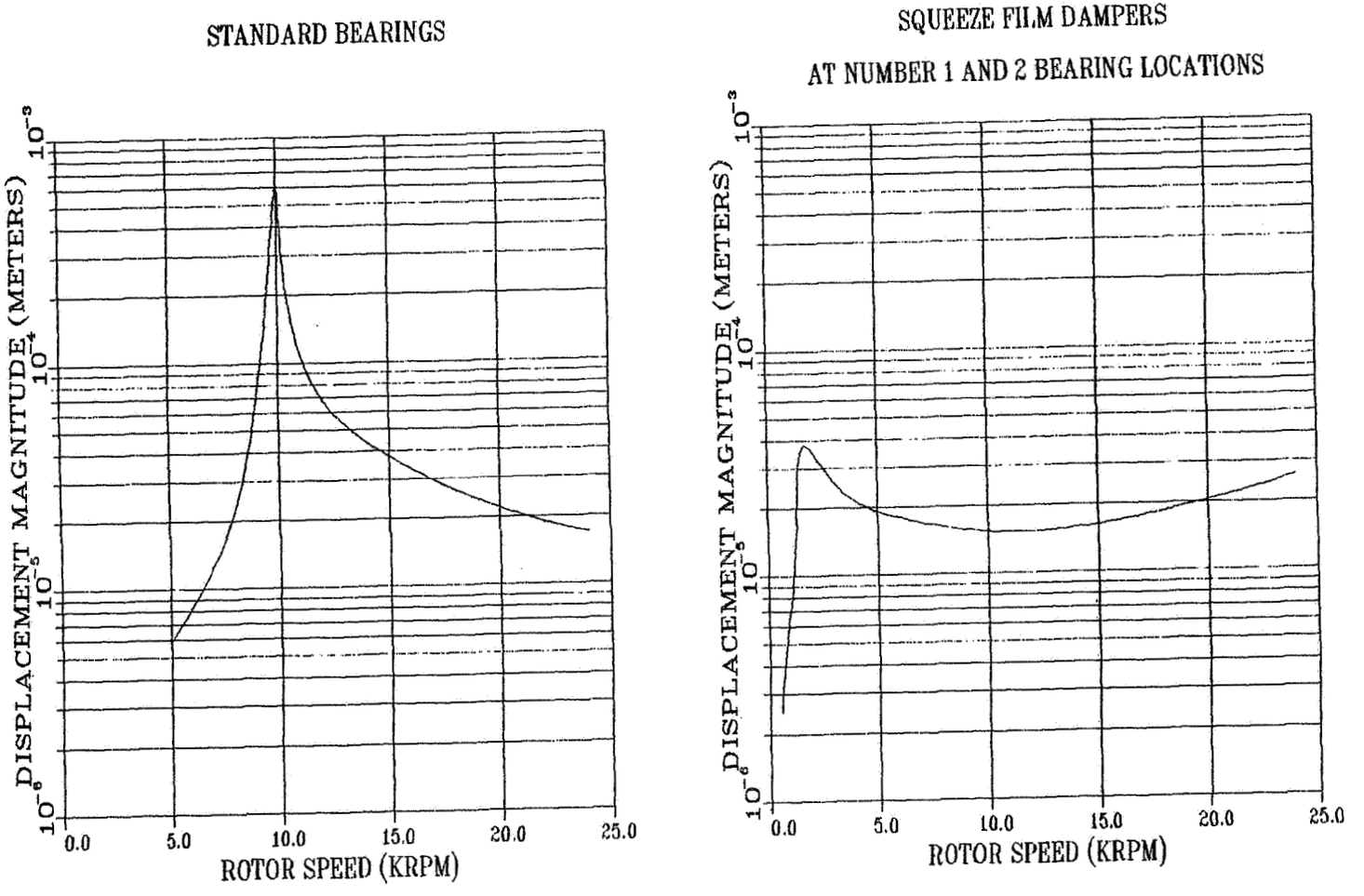

Figure 17. - Power rotor system response at spline 1 as predicted by steady state analysis.

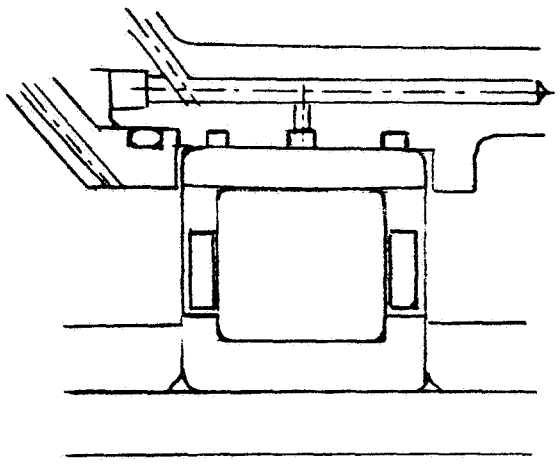

Figure 18. - Squeeze film damper applied to roller bearing.